Effects of Boulders on Bed Morphology and Hyporheic Flow

A Thesis

Presented in Partial Fulfillment of the Requirements for the

Degree of Master of Science

with a

Major in Water Resources

in the

College of Graduate Studies

University of Idaho

by

Taylor J. Dudunake

Major Professor: Daniele Tonina, Ph.D.

Committee Members: William Reeder, Ph.D.; Elowyn Yager, Ph.D.; Stephen Hundt, M.S.

Department Administrator: Timothy E. Link, Ph.D.

December 2020

Authorization to Submit Thesis

This thesis of Taylor J. Dudunake, submitted for the degree of Master of Science with a Major in Water Resources and titled "Effects of Boulders on Bed Morphology and Hyporheic Flow," has been reviewed in final form. Permission, as indicated by the signatures and dates below, is now granted to submit final copies to the College of Graduate Studies for approval.

Major Professor: ______________________ Date: 11/19/2020
Daniele Tonina, Ph.D.

Committee Members: William Jeffery Reeder Date: 11/19/2020
William Reeder, Ph.D.

______________________ Date: 11/18/20
Elowyn Yager, Ph.D.

STEPHEN HUNDT Digitally signed by STEPHEN HUNDT Date: 2020.11.19 10:10:43 -07'00' Date: 11/19/2020
Stephen Hundt, M.S.

Department Administrator: Timothy E. Link Date: November 23, 2020
Timothy E. Link, Ph.D.

Authorization to Submit Thesis

This thesis of Taylor J. Dudunake, submitted for the degree of Master of Science with a Major in Water Resources and titled "Effects of Boulders on Bed Morphology and Hyporheic Flow," has been reviewed in final form. Permission, as indicated by the signatures and dates below, is now granted to submit final copies to the College of Graduate Studies for approval.

Major Professor: ______________________________________ Date: ___________
Daniele Tonina, Ph.D.

Committee Members: ______________________________________ Date: ___________
William Reeder, Ph.D.

______________________________________ Date: ___________
Elowyn Yager, Ph.D.

______________________________________ Date: ___________
Stephen Hundt, M.S.

Department
Administrator: ______________________________________ Date: ___________
Timothy E. Link, Ph.D.

Abstract

Stream hydromorphology regulates instream water flow and interstitial flow of water within streambed sediments, the latter known as hyporheic exchange. Whereas hyporheic flow has been studied in sand-bedded streams with ripples and dunes and in gravel-bedded streams with pool-riffle morphology, little is known about its characteristics in plane bed morphology with subdued streambed undulations and sparse macro-roughness elements such as boulders and cobbles. Here, we present a proof-of-concept investigation on the role of boulder-induced morphological changes on hyporheic flows based on coupling large-scale flume sediment transport experiments with computational fluid dynamics. Our results show that placement of boulders on plane beds increase the reach scale hyporheic median residence time, τ_{50}, by 15% and downwelling flux, q_d, by 18% from the plane bed. However, reach scale hyporheic exchange changes are stronger with τ_{50} decreasing by 20% and q_d increasing by 79% once the streambed morphology reached equilibrium (with the imposed upstream sediment and flow inputs on boulders). These results suggest that hyporheic flow is sensitive to the geomorphic response from bed topography and sediment transport in gravel-bedded streams, a process that has been overlooked in previous work.

Acknowledgements

My deepest appreciation goes to the University of Idaho Center for Ecohydraulics Research for providing me a quality education and unique graduate school experience. Specifically, I'd like to thank my advisor, major professor, and mentor Dr. Daniele Tonina for his patience and guidance throughout my graduate school experience. Similarly, Dr. Jeff (William) Reeder provided me the necessary background knowledge in the computation modeling of hyporheic flow and much appreciated guidance while Dr. Tonina was on sabbatical. Also, thank you to Angel Monsalve who provided critical assistance in the publication process of our Water Resources Research journal article. Finally, my colleagues at the U.S. Geological Survey Idaho Water Science Center deserve my deepest appreciation as they remained patient and supportive of me while I was working as a Pathways Student Hydrologist throughout the duration of my degree program at University of Idaho.

Dedication

This work is dedicated to my parents, Harry and Ilene, and partner in life, Hailey. This would not have been possible without your love and support. I thank you three from the bottom of my heart for allowing me to pursue my dreams and admiration of the natural world.

Table of Contents

List of Tables

List of Figures

Statement of Contribution

The journal article titled "Local and Reach-Scale Hyporheic Flow Response From Boulder-Induced Geomorphic Changes" was submitted and approved for publication in *Water Resources Research* in October 2020. This thesis is a result of that publication for which I, Taylor Dudunake, was the lead-author and researcher with collaboration from Daniele Tonina, William Reeder, and Angel Monsalve. The primary collaborative efforts by those co-authors included experimental oversight and guidance, along with background knowledge of the initial dataset used in these experiments.

Chapter 1: Local and Reach-Scale Hyporheic Flow Response From Boulder-Induced Geomorphic Changes[1]

Introduction

Channel morphology and bedform dynamics play a critical role for hydrological processes that span a wide range of spatial and temporal scales surrounding riverine environments (Malard et al., 2002; Stanford et al., 2005; Stanford & Ward, 1988). These processes regulate stream and river hydrodynamics (Leopold & Wolman, 1957) and the surrounding ecosystem (Krause et al., 2017; Stanford & Ward, 1993) and influence the characteristics of hyporheic exchange (i.e., the process in which stream water flows within the interstices of streambed sediments thus forming the hyporheic zone) its occurrence rate (Boano et al., 2014; Boulton et al., 2010; Kasahara & Wondzell, 2003). River channels may take different geomorphic forms as a result of sediment and flow regimes and local characteristics, e.g., vegetation, sediment size and distribution, and biotic activities (Buffington & Montgomery, 2013; Rosgen, 1994). River's hydromorphological characteristics will impact not only surface hydraulics (Julien, 2002), but also the surface water interaction within the hyporheic zone (Boano et al., 2014). Spatial variability in hydrodynamic characteristics often result in changes to the bed surface, which determines hydraulic head gradients (Kasahara & Wondzell, 2003; Pryshlak et al., 2015), which in turn controls the pumping process of hyporheic flow in and out of the bed (Cardenas & Wilson, 2007; Elliott & Brooks, 1997; Harvey, Judson W., Gooseff, 2015). Given that hyporheic exchange characteristics are primarily controlled by the hydraulic head gradients, the spatial scale at which hyporheic exchange is studied must be considered (Gooseff, 2010; Magliozzi et al., 2018; Stonedahl et al., 2010).

Most research on hyporheic exchange has focused on hyporheic hydraulics of well-defined periodic bedforms (Boano et al., 2014) such as dune-like morphology (Cardenas et al., 2004; Elliott & Brooks, 1997; Harvey & Bencala, 1993; Janssen et al., 2005; Marion et al., 2002; Packman & Brooks, 2001; Zaramella et al., 2003), three-dimension dunes (Chen et al., 2018), pool-riffle morphology (Marzadri et al., 2010; Tonina & Buffington, 2007; Trauth et al., 2013), and meander bends (Boano et al., 2010; Cardenas, 2009). Fewer investigations looked at the impact of single structures such as spanning logs (Sawyer et al., 2011), low-head weirs (Briggs et al., 2013; Endreny et al., 2011; Hester & Doyle, 2008; Smidt et al., 2015), or large sparsely distributed particles (Hutchinson & Webster, 1998). Many of these studies are purely numerical simulations and do not

[1] "Local and Reach-Scale Hyporheic Flow Response From Boulder-Induced Geomorphic Changes" published in *Water Resources Research*, vol. 56, issue 10, 2020

account for feedback between structures (e.g., macro-roughness elements) and streambed morphology changes due to sediment transport (e.g., scour and depositional areas). Similarly, limited research is available on hyporheic mechanisms in other bedforms such as a plane bed river with subdued undulations and randomly spaced boulders and cobbles (Montgomery & Buffington, 1993). These stream reaches are common in the upper part of the fluvial network where hyporheic processes are expected to be important (Payn et al., 2009). These stream reaches have key implications for salmonid species such as bull trout and salmon which spawn in hyporheic sediments where habitat quality is of great importance (Zimmermann & Lapointe, 2005) and biogeochemical reactions are abundant (Marzadri et al., 2017) due to high streambed permeability and vertical connectivity.

Here, we present a proof-of-concept investigation and a conceptual framework that accounts for the feedback between macro-roughness elements (e.g., boulders, logs, vegetation, and streambed morphology) and their overall impact on hyporheic exchange. This work aims to understand the role of macro-roughness elements and subsequent morphological changes (e.g., scour and deposition), and their effect on hyporheic exchange. We hypothesize that boulders induce morphological changes (e.g., scour and depositional zones on the bed), which enhance hyporheic exchange to a greater degree than the isolated effect of the presence of boulders (Figure 1).

We believe that the related morphological changes, which are a function of flow, sediment regime, local grain size characteristics, and macro-roughness size, chiefly control the hyporheic exchange induced by the boulders. Plane bed streams are characterized by a lack of coherent topographical features even though they may have small depressions and humps due to sediment transport (Montgomery & Buffington, 1993) (Figure 1a). These small undulations on the streambed may induce shallow hyporheic flows that can be further enhanced by placing large boulders on the streambed, a common practice used in stream restoration (Figure 1b) (Abbe & Brooks, 2011; Branco et al., 2013; ODFW, 2010; Thompson & Stull, 2002). However, we posit that post-placement interactions between macro-roughness elements (boulders) and flow hydraulics and sediment flux will, over time, alter the streambed morphology, further enhancing hyporheic exchange (Figure 1c). Generally, flow obstructions generate local flow constriction points at localized areas in a stream. This process results in higher surface flow velocities and increased sediment transport capacity and hydraulic head gradients. The overall effects that boulders have on fluvial geomorphology play a direct role on sediment transport. Areas of erosion and deposition can be expected in the vicinity of structures after changing flow characteristics from in-stream restoration practices following various spatial and temporal patterns (Figure 1c). These geomorphic responses can occur throughout different various spatial locations and temporal instances and will evolve over time due to sediment input and high flow (sediment mobilizing) history.

Thus, the objective of this study was to quantify how hyporheic exchange patterns change following a geomorphic response produced by macro-roughness elements (Figure 1). We used large-scale flume experiments that modeled the sediment transport in a plane bed stream with large boulders. The flume experiments provided the plane bed, and the pre- and post-sediment transport topographies with boulders. The topographies were used in detailed surface flow Large Eddy Simulations (LES), which quantified and provided the hydraulic head distribution as boundary conditions for a groundwater model that simulated hyporheic flow. Using the groundwater models, we examined (1) the spatial properties of hyporheic flow, (2) the volume of hyporheic exchange, and (3) the residence time distribution of water in the hyporheic zone for three scenarios. Our studied scenarios were a) plane bed without boulders, b) plane bed with evenly spaced boulders before the streambed adjusted to the imposed flow conditions, and c) the observed response to one set of flow and sediment supply conditions (equilibrium conditions, see section 2.1 for details). Different geomorphic responses will be observed for different hydraulic and sediment supply scenarios (Monsalve et al., 2017). However, the pattern of erosion and deposition is generally consistent (i.e., deposition upstream of the boulder and erosion downstream).

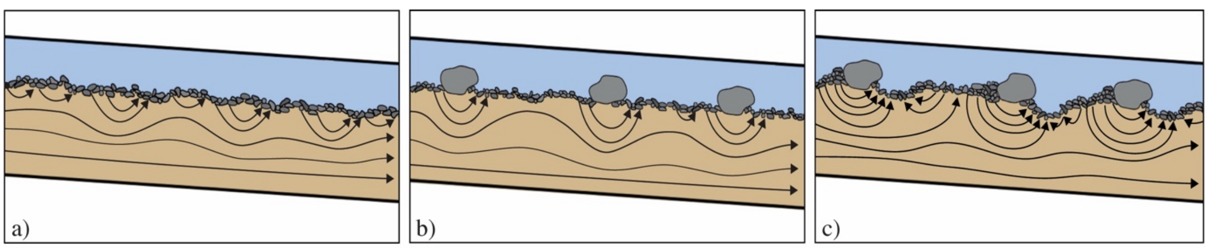

Figure 1. Conceptual representation of hyporheic exchange for a a) plane gravel streambed without boulders, b) plane gravel streambed with evenly spaced boulders before the streambed adjusted to the imposed flow and sediment input, and c) after the geomorphic response on the streambed. Black lines represent flowpaths and the general direction of travel in the subsurface sediments. Surface flow direction is left to right.

Methods

Experimental Description and Bed Topography

We based our analysis on a set of experiments described in Monsalve et al. (2017) initially designed to capture the dynamics of surface flow on sediment transport dynamics around boulders. We related these dynamics to the hyporheic exchange process in streams where relatively large immobile boulders are present. All our experiments were conducted at the Center for Ecohydraulics Research StreamLab, University of Idaho (Budwig & Goodwin, 2012) in a 0.76 m wide and 20 m long channel with a bed slope of 2.15% and constant discharge, Q = 0.0596 m^3/s. Average flow depths fluctuated between 7.7 cm and 8.2 cm. To simulate boulders in a natural stream environment, the flume experiment contained staggered immobile concrete hemispheres with a diameter (D) of 15.24 cm. The distance between hemispheres (λ) was 61 cm ($\lambda/D \approx 4$), and the hemisphere concentration was ~0.05 (A_D/A_T, area occupied by hemispheres divided by total bed area). These ratios were within the range of previously observed values, $0 \leq A_D/A_T \leq 0.4$ (Nitsche et al., 2011), and those used in flume experiments, $1 \leq \lambda/D \leq 5$ (Yager et al., 2007). This staggered configuration and density corresponded to an isolated flow regime with no interfering wakes between consecutive boulders (Strom et al., 2007). At the beginning of the experiment the bed consisted of a 10 cm thick sediment layer with median (D_{50}) and 84th percentile grain size (D_{84}) of 10 mm and 19.8 mm, respectively. The ratio between D of the boulder and D_{84} of the sediment was also consistent to those found in natural streams (Nitsche et al., 2011).

Our experiment started with a relatively plane bed with the staggered boulder configuration (Figure 2b). We let the bed adjust to the imposed flow conditions and upstream sediment supply ($q_s = 0.6$ kg/s), which corresponds to at capacity sediment transport, until equilibrium conditions were reached (Figure 2c). We defined equilibrium conditions as the instance when the mean bed and water surface slopes were no longer changing, reach-averaged velocity was constant, the upstream sediment supply was equal to the total transport capacity, and the grain size distribution exiting the flume was identical to that of the upstream supply. Hereinafter, we refer to the experimental morphological condition such that initial and final bed states correspond to the plane gravel bed with boulders at the beginning and once equilibrium conditions were reached, respectively. We surveyed the bed topography for initial and final bed states under dry conditions using a high-speed (50 kHz), high-accuracy (about 0.1 mm) charge-coupled device, laser displacement scanner to determine the bed elevation with a resolution of 5 mm x 5 mm. Digital elevation models (DEMs) were developed after scanning the bed topography. To quantify the magnitude of changes in bed surface elevation and determine areas of erosion and deposition we constructed a DEM of difference by subtracting the initial bed elevations from the final bed elevations (Figure 2d). Knowing where depositional and erosional areas exist on the bed surface was useful for understanding how bed topography affected the spatial properties of hyporheic flow. Specific details related to bed structure, flow conditions, and experimental methodology can be found in Monsalve et al. (2017).

Surface Flow Modeling and Spatial Distribution of Bed Surface Hydraulic Head

Modeling the groundwater flow requires a spatial distribution of the hydraulic head over the area of interest. In our case, given the experimental conditions (i.e., relatively high longitudinal slope, rough gravel bed, roughness elements, and erosional and depositional landforms), the local bed elevation, water surface elevation, and velocity varied dramatically. Therefore, a complete characterization in space and time of the hydraulic head distribution based solely on measured variables was not viable. To obtain the hydraulic head distribution in our experiments, we relied on surface hydraulic modeling (Tonina & Buffington, 2009; Trauth et al., 2013) and used a coupled LES – Volume Of Fluid model. LES is a highly sophisticated turbulence model that solves the spatially filtered Navier-Stokes equations integrated over time at the scale of a finite volume grid and captures small-scale flow features. The Volume of Fluid (VOF) is a free-surface modelling technique used for tracking and locating the free surface. This coupled approach was necessary for characterizing hydraulic head. LES allowed us to explicitly consider local and macro-roughness effects, such as bedforms, obstructions, individual surface grains, and small-scale bed elevation features by using a grid cell resolution of 0.5 mm. VOF was required because the water depth over the boulders was too shallow (plunging flow) or varied dramatically within the experimental area. Given the sharp gradients in water surface elevation, other techniques to define the location of the upper boundary in our model such as the rigid lid are not appropriate (Kang et al., 2016; Khosronejad et al., 2013, 2015; Monsalve et al., 2017). In all our calculations, the system of equations were solved using the OpenFOAM® (www.openfoam.org) flow solver interFoam (Weller et al., 1998).

Three numerical models were developed to characterize the hydraulic head for plane bed conditions without boulders and the initial and final bed conditions with boulders (surveyed from the flume experiments). The first experiment characterizes the plane bed using a simplified version of the initial bed conditions. This model was based on the initial bed state, but the concrete hemispheres were digitally removed from the bed topography and filled with nearby bed elevations (Fig 2a). In the process, some artificial transitions appeared at the boundaries of the removed boulders. We applied a smoothing filter (approximately 1 cm in width, equal to the D_{50}) to minimize the sharp non-natural gradients nearby the removed boulders. The goal of this scenario was to isolate the effect of boulders in the distribution of hydraulic head and consequently in the hyporheic flow. Hereinafter, we refer to this condition as the original plane bed. The second experiment (initial bed state) corresponds to the bed topography at the beginning of the flume experiment where no macro-bedforms were present other than concrete hemispheres (Figure 2b). The third experiment (final bed state) corresponds to the bed topography at the end of the flume experiment once equilibrium conditions occurred (Figure 2c). To reduce the computational time required to conduct each simulation our numerical domain was reduced to 6 m long from the original 20 m length of the Mountain StreamLab. Within this length we included a study section ($3.4<X<6.4$ m; hereinafter, X, Y, Z are the streamwise, cross-stream, and vertical directions in the flume, respectively) with three sequences of hemispheres (Figure 2d), upstream ($1.4<X<3.4$ m) two sequences of boulders upstream of the study section, and one sequence of boulders downstream to remain consistent with the roughness elements ($6.4<X<7.4$m). The two upstream boulder sequences were used to ensure fully developed turbulent flow in the study section and the single downstream sequence, which simulated the flume's tailgate, was used to control the water surface elevation. Once the flow was well established within the flow model domain (i.e., flow discharge at the outlet was in average equal to the inlet) and after we conducted a convergence analysis we let the LES run for 60 seconds and then calculated the time-averaged distribution of hydraulic head on the bed surface.

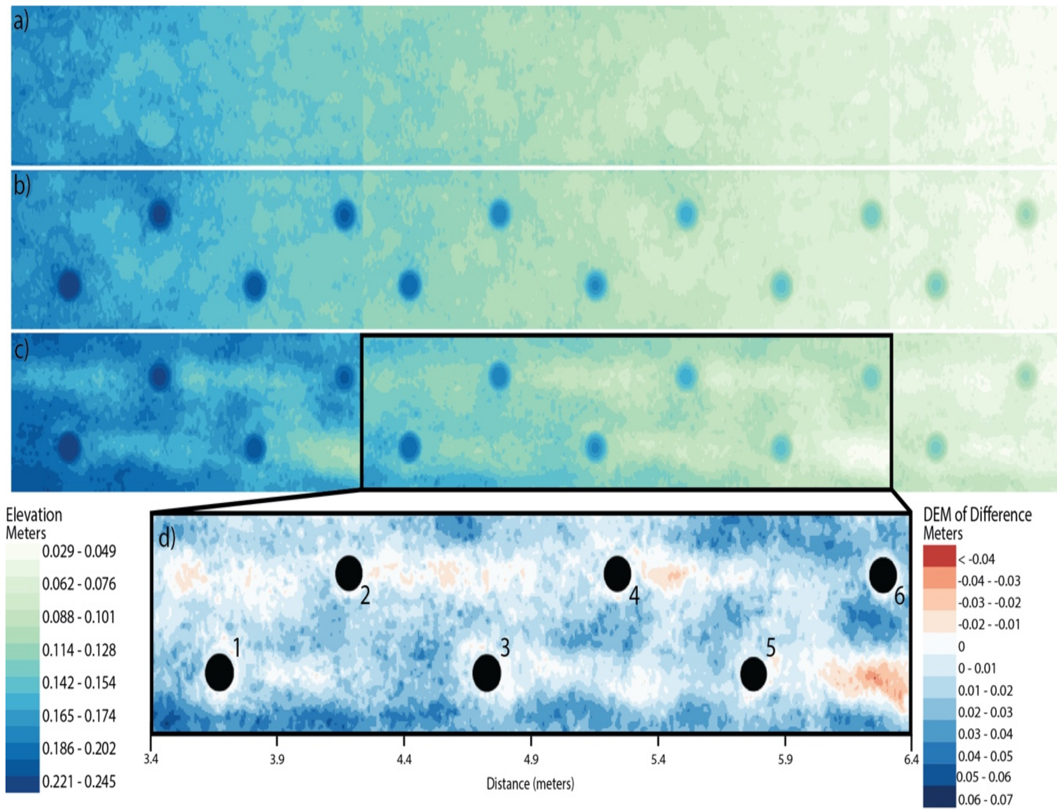

Figure 2. Spatial distribution of bed elevation for a) original plane bed, b) initial bed state (plane gravel streambed with evenly spaced boulders before the streambed adjusted to the boulders) and c) final bed state (the same plane gravel streambed with evenly spaced boulders after the geomorphic response on the streambed). d) DEM of difference for the study section highlighting erosion (red/warm) and deposition (cold/blue) regions. Numbers indicate the boulder identification number. Flow direction is left to right.

Bed Morphology and Hydraulic Head Properties

The LES-VOF model allowed us to characterize the time-averaged distribution of hydraulic head in all our experiments. We used this data as input to quantify the distribution of subsurface hydraulic head using the modular finite-difference flow model (MODFLOW 2005) in the Groundwater Modeling System (GMS) software package (Aquaveo L.L.C., 2019; Harbaugh, 2005). MODFLOW is a widely used numerical model that solves the groundwater flow equations through porous subsurface material. Other studies have used MODFLOW to examine various hyporheic properties (Hester et al., 2019; Storey et al., 2003).

To quantify the effects of bed morphology on hyporheic exchange and to solve for the subsurface hydraulic head distributions in each bed condition scenario we used MODFLOW. Our subsurface numerical models were 5.99 m long, 0.67 m wide, and 0.5 m deep with 16,186,500 cells at a resolution of 0.005 m in the X, Y, and Z directions. To avoid upstream and downstream edge effects and ensure fully developed hyporheic flow we only used the numerical data obtained in the LES-VOF model within the study section in this analysis (Figure 2d, 3.4 m $\leq$ X $\leq$ 6.4 m). Hydraulic head on the top, upstream, and downstream boundaries were defined as constant heads, allowing for a desired gradient along the domain. No-flow boundaries were assigned to the bottom and walls of the domain. The hydraulic head distribution from the surface flow model was assigned to the top boundary. We used a homogenous and isotropic hydraulic conductivity (*K*) of 0.01 cm/s, with uniform porosity of 0.3, which are within the range of previously observed values (Malcolm et al., 2004; Sebok et al., 2015). We assigned *K*=0 cm/s at each boulder because they are impermeable in the initial and final scenarios.

To determine the effects of morphology on hyporheic exchange and subsurface residence time distributions (RTD), we used MODPATH, a post-processing particle-tracking program, to determine spatial and temporal properties of hyporheic flowpaths (Pollock, 2012). Residence time is defined as the time necessary for a water particle to travel through the subsurface along a flowline. We investigated the properties of the flowpaths on the reach-scale (2 m^2) and at a local-scale (0.4 m^2) immediately surrounding the boulders in each scenario. The reach-scale analysis investigated all the cells in the model domain encompassed by the study section. Because a majority of the hyporheic flow travels in the streamwise direction, we defined the boulder-scale analysis within the area extending a distance of one boulder diameter upstream and downstream and 0.5x boulder diameter in the cross-stream direction in all cases. This area captures the morphological changes on the bed near the boulder and the boulder-scale effects of hyporheic flow. Given that it is unclear at what elevation the streambed is located in a gravel bed and thus where hyporheic flows start, we based our choice on observations conducted in field studies and define it based on the armor layer thicknesses of gravel beds, which is typically two times the D_{50} (Tonina & Buffington, 2007). Therefore, we distributed seeding particles at this depth (2.5 cm) in the downwelling portions (corresponding to the fifth layer of the MODFLOW simulation) throughout the study area of each scenario. Seeding particles are used to quantify and conceptualize the movement of water through the subsurface sediments. For the purposes of this study, we call the fifth layer the hyporheic surface. The downwelling flux in each cell on the hyporheic surface was determined from the particle motion in the MODFLOW solutions. Residence time was calculated only for seeding particles that returned to the hyporheic surface and stayed within the model domain. Less than 2% of the particles left the domain at the downstream boundary.

From the results of the RTD analysis, we determined the mean, median, and standard deviation of the flux-weighted residence time distribution. Hereinafter, residence time is weighted by downwelling flux. Also, we calculated the total downwelling area (i.e., sum of all downwelling cells area on the hyporheic surface) and hyporheic discharge (i.e., product of average downwelling flux and total downwelling area) to determine how hyporheic exchange differs among the scenarios.

Additionally, we calculated the mean and maximum hyporheic flow depth and hyporheic volume, which is the maximum theoretical volume between the surface enveloping all the hyporheic flow and the streambed surface (Cardenas & Zlotnik, 2003). Finally, to understand the spatial extent of hyporheic exchange in each scenario, we calculated hyporheic area as the total area on the hyporheic surface where any flowline existed in the subsurface directly below.

Results and Discussion

Bed Morphology and Surface Hydraulic Head Properties

The original plane bed configuration was characterized by low-amplitude streambed undulations and was without boulders. Similarly, the initial plane bed was featureless only with boulders prior to sediment transport. Conversely, the final plane bed had extensive areas of sediment deposition and erosion. Maximum vertical elevation changes from the initial plane bed were similar in magnitude (7 cm) to the boulder radius (Figure 2d). Depositional areas primarily occurred upstream of the boulders and alternating sides along the walls (2 cm on average) while erosional areas were observed between consecutive boulders. Less energy along the walls of the flume encouraged sediment deposition to occur providing an ideal location for seeding particles to enter the streambed as hyporheic flow. Elongated pool-like areas formed downstream of the boulders as a result of local bed scour caused by plunging flow imposed by the boulders. Similar geomorphic responses have been observed for emerging bed structures such as bridge piers and vegetation (Ettema et al., 2006; Yager & Schmeeckle, 2013). In general, none of the boulders were fully buried at equilibrium. There was a net reach-averaged sediment accumulation on the bed surface of 8.1×10^{-3} m^3/m. The grain size distribution of the surface sediment of the initial and final bed state were not statistically different, similar to Monsalve and Yager (2017). An explanation of the processes behind the bed surface adjustments is beyond the scope of this study. Specific details of the mechanics of bed changes for this and similar experiments are described in Monsalve and Yager (2017).

Each bed configuration (i.e., original, initial, and final plane bed) generated different surface, bed-surface hydraulic head distributions (Figure 3), and hyporheic flow patterns (see section 3.2). In each scenario, high and low head areas generally coincided with higher and lower bed elevations, respectively. However, the trends were slightly different around the boulders. High and low head were observed immediately upstream and downstream of the boulders, respectively, whereas the lowest hydraulic head were near the boulder tops where water depth shallowed. The addition of boulders increased the local maximum hydraulic head by 0.31 m (expressed in meters of water) from the original plane bed scenario and by 0.38 m after the geomorphic response. We observed the largest increase in maximum head near boulders 2 and 4 once the bed morphology adjusted to the surface flow imposed by the boulders. These head variations created gradients that forced hyporheic flow in the downstream direction throughout the study section and near each boulder.

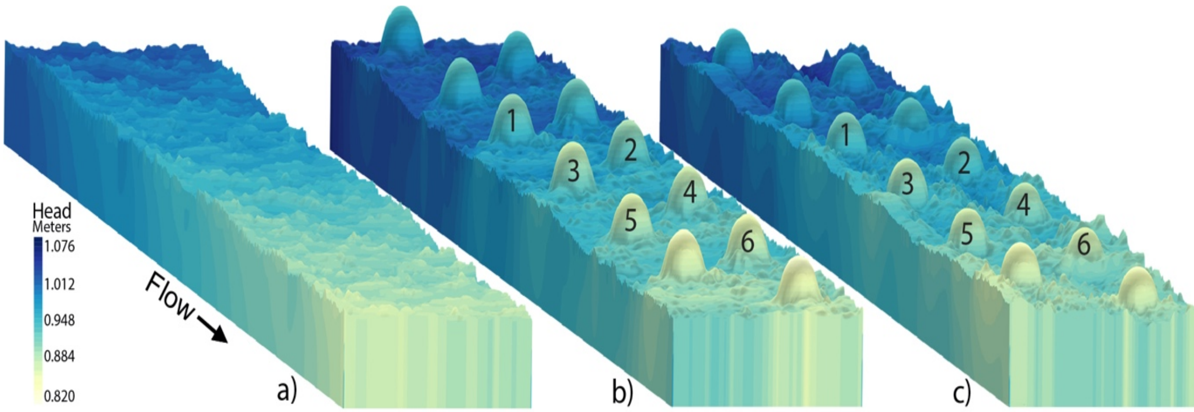

Figure 3. Spatial distribution of bed elevation and hydraulic head (colored scheme) for a) original b) initial, and c) final plane beds.

Reach-Scale Hyporheic Flow

We observed trends in spatial properties of hyporheic flow throughout the study section of each scenario (summarized in Table 1).

Table 1. Summary of Reach-Scale Hyporheic Modeling

Experiment	τ_{mean} (hr)	τ_{50} (hr)	σ_τ(hr)	q_d[b](cm/hr)	A (ratio)	Q_h (cm^3/s)	V_h (m^3)	D_{max}(cm)
Plane Bed	4.77	0.71	13.14	-11.19	0.51	31.2	0.31	36.51
Initial[a]	3.49	0.82	6.97	-13.24	0.52	36.2	0.38	37.72
Final[a]	3.11	0.57	8.43	-20.08	0.48	52.7	0.39	42.41

Note: Symbols are flux-weighted mean residence time (τ_{mean}), flux-weighted median residence time (τ_{50}), flux-weighted standard deviation of residence time (σ_τ), mean downwelling flux (q_d), ratio of downwelling area to total area (A), hyporheic discharge (Q_h), hyporheic volume (V_h), maximum hyporheic depth (D_{max}).
[a]Initial and Final indicate the bed condition for the plane bed with boulders before and after sediment transport, respectively. [b]Negative values indicate flux in the downward direction.

Reach-Scale Residence Time

Mean hyporheic residence time exhibited a decreasing trend as the morphologic changes acted on the bed surface. The overall limited variability in hydraulic head and topography in the original plane bed scenario without boulders resulted in hyporheic residence times that were on average longer and more variable around the mean residence time than in other scenarios. The variability in head and topography that drives hyporheic flow increased in the ffinal scenario relative to the initial scenario based on the standard deviation of residence time. The boulders and modified bed surface in the final scenario generated faster and shallower flowpaths on average, which resulted in a shorter mean and median residence time. The increased residence time variability in the final plane bed scenario was the result of areas of deposition and erosion around the boulders which increased the range in hydraulic head as also shown by the variability in flow line lengths. The mean residence time was relatively longer than the median residence time in each scenario. However, τ_{50} increased from the original plane bed to the initial plane bed scenario but decreased to the final plane bed. As the streambed transitions from the original plane bed to the initial plane bed with boulders and then to the final plane bed in equilibrium, the residence time distribution becomes narrower with less variability (i.e. smaller standard deviation, Table 1). The flux-weighted residence time distributions had a similar shape for each bed scenario. In particular, a lognormal distribution may be considered a relatively good first approximation of the spatial distribution of residence time in each bed scenario (Figure 4). According to the Kolmogorov-Smirnov (K-S) goodness-of-fit test (95% confidence), the initial plane bed scenario is well-described by the lognormal distribution. In the original plane bed and final bed scenarios we predicted values of 0.0236 and 0.0113, respectively, whereas the critical threshold is 0.0068 (95% confidence). Therefore, a lognormal distribution may be used only as a rough estimation.

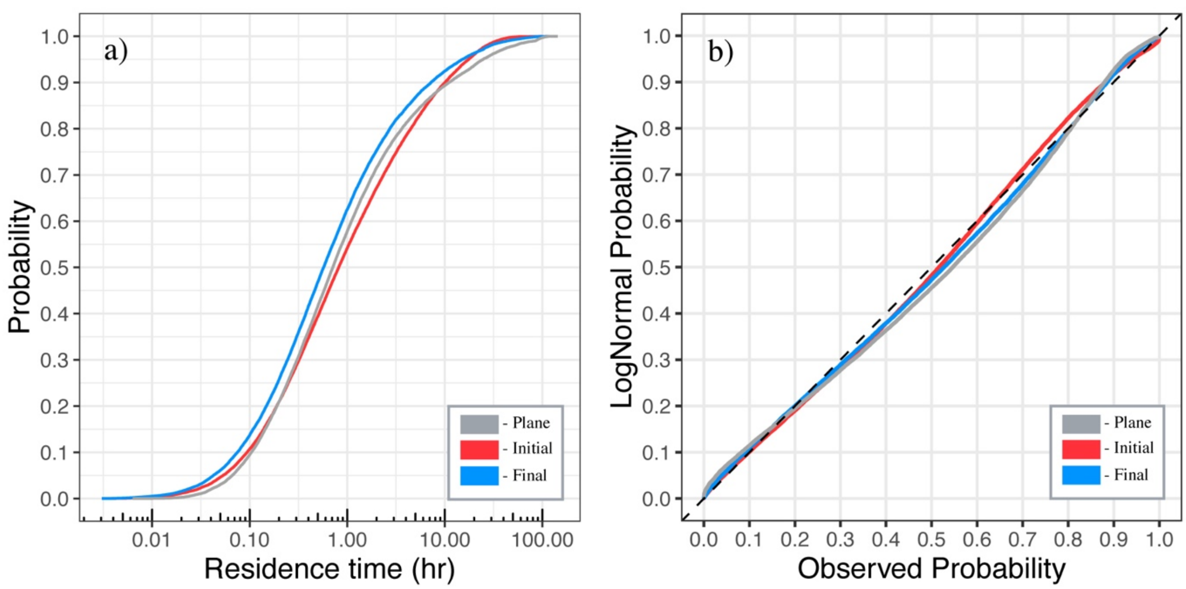

Figure 4. Cumulative probability distribution of flux-weighted residence times for different bed morphologies. A lognormal distribution is considered a good first approximation of the residence time distribution for original, initial, and final plane bed scenarios. The cumulative distribution function of residence time showed a small deviation between distributions of each scenario (a). A lognormal distribution plotted as a straight line on a normal probability plot (b).

Reach-Scale Hyporheic Flow Spatial Characteristics

Reach-scale hyporheic flow simulations not only show the effect bed morphology has on residence time and flux of hyporheic flow, but also the associated spatial variability (Figure 5). Hyporheic flowpaths for the original plane bed are chaotic without a systematic pattern (Figure 5a). A systematic pattern is visible in the initial bed where the boulders dominate the formation of hyporheic flow (Figure 5b). The formation of erosional and depositional areas in the final bed scenario reintroduces part of the chaotic behavior (Figure 5c) of the original plane bed which increased the residence time variability (σ_τ). These data indicate bed morphology has a noticeable effect on the mean downwelling flux, the area on the bed where downwelling occurs, and the depth of hyporheic flow in the study section of each scenario.

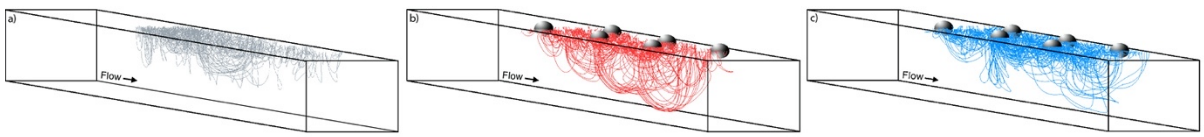

Figure 5. Effects of hydraulic head and topography in downwelling hyporheic flow. Modeled flowpaths show how downwelling hyporheic flow moves through the subsurface in the presence of boulders. Spatial hyporheic flow characteristics change as a consequence of morphologic changes on the bed surface surrounding boulders. Particle-tracking was used to model flowpaths for original plane bed (a), initial (b), and final (c) bed conditions. For simplicity, these figures represent a portion of the total flowpaths used in the analysis.

The calculated mean downwelling flux in the initial and final scenarios captured the effect boulders have on hyporheic flow. The downwelling flux of hyporheic flow in the final bed scenario was faster than in the other scenarios. This result suggests that boulders alter the surface flow characteristics, but also affect hyporheic flow more than we originally thought. The changes in surface flow characteristics result in adjustments to bed topography due to boulder-induced increases in near-bed shear stresses and associated head distributions, which increased the hyporheic downwelling flux and decreased the hyporheic mean residence time. The total downwelling area on the bed surface decreased more in the final scenario, after the bed topography adjusted to the flow characteristics imposed by the boulders, relative to the initial bed condition. This observation suggests morphologic changes also influence the spatial characteristics of hyporheic flow. Examination of hyporheic flowpaths showed flow traveling deeper in the subsurface of the final scenario compared to other scenarios. These flowpaths make up the tails of the residence time distribution because a majority of the hyporheic flow was concentrated closer to the bed surface with greater downwelling velocities and shorter residence times. Although the downwelling area was smaller in the final scenario, the total hyporheic exchange substantially increased as a result of the greater mean downwelling flux. Because of this observed relationship between downwelling area, hyporheic exchange, and mean downwelling flux, we can verify that mean residence times in the final scenario were the shortest. The maximum hyporheic volume was the largest in the final scenario. This indicates that bed morphology also influences the volume of water in the subsurface from hyporheic flow.

Data from these simulations show how increasing bed complexity similar to the final scenario affects the residence time, spatial properties, and flux of hyporheic flow. To summarize, more hyporheic flow entered the subsurface at higher downwelling velocities and spread across a smaller bed surface area resulting in a larger volume per unit time after the bed adjusted to macro-roughness elements. Despite 3% of the reach-scale bed surface being blocked by impermeable boulders, downwelling flux and hyporheic discharge increased in the final scenario due to the morphological changes and increased hydraulic gradient imposed by the boulders. This observation also indicates that hyporheic flow is sensitive to changes in bed morphology induced by structures that obstruct flow in a stream.

Boulder-Scale Hyporheic Flow

Comparison of hyporheic flow properties in the area surrounding individual boulders (boulders 1-5, Figure 2) for two distinct bed scenarios reveals that bed morphology influences hyporheic flow in regions near boulders. Boulder-scale hyporheic flow properties were similar to observed trends in the reach-scale analysis. These properties were not calculated for boulder 6, because they may be influenced by the downstream boundary condition (Table 2).

Boulder-Scale Residence Time

Hydraulic head gradients near boulders directly influence how long hyporheic flow stays in the subsurface as it downwells under the boulders. The mean hyporheic residence time decreased between initial and final scenarios at three boulders (1, 3, 4) and increased at two boulders (2, 5). We calculated the median residence time to better understand how bed morphology surrounding boulders influence the movement of hyporheic flow. The median residence time decreased for all boulders from initial to final scenarios and was always shorter than the mean residence time. The latter suggests the presence of few long residence times at the tail of the distribution. This is partly due to the increased head gradient along the stream-wise direction of the boulders from deposition and erosion. The standard deviation of residence times suggests that morphological changes near the boulders created more variable hyporheic flow at four boulders (2, 3, 4, 5) but less variable hyporheic flow at one boulder (1). The biggest variability in observed residence times occurred in the final scenario at boulder 2. These data indicate that morphological changes have widely distributed spatial effects on hyporheic flow in the study section. The observed residence times of hyporheic flow near the boulders were also lognormally distributed as they were in the reach-scale residence time analysis and satisfied the K-S goodness-of-fit test for each scenario with a 95% confidence level (Figure 6).

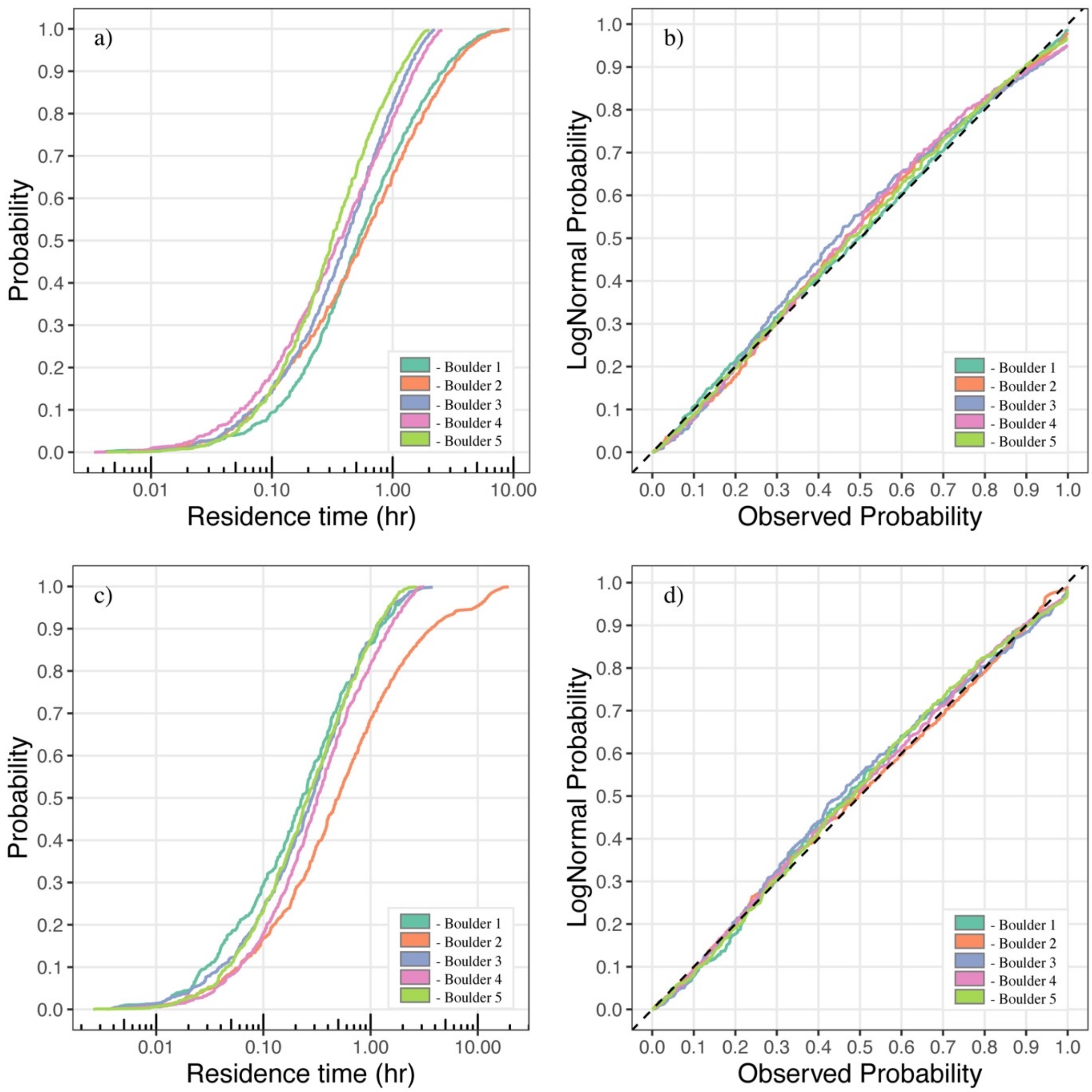

Figure 6. Probability of occurrence of residence time for different bed morphologies. Residence time distribution near boulders for two bed scenarios closely follow a normal distribution. The cumulative distribution function of residence time shows a small deviation of distribution between initial and final scenarios, respectively (a, c). A lognormal distribution plots as a straight line on a normal probability plot for initial and final scenarios, respectively (b, d). The residence time probabilities are lognormally distributed in each scenario.

Table 1. Summary of Boulder-Scale Hyporheic Modeling

Boulder	Bed condition	τ_{mean} (hr)	τ_{50} (hr)	σ_τ(hr)	$q_d{}^b$(cm/hr)	A (ratio)	Q_h (cm^3/s)	V_h (cm^3)	D_{max}(cm)	D_{mean}(cm)	A_h(cm^2)
1	Initial	1.02	0.52	1.27	-23.13	0.43	1.24	4224.3	16.6	9.51	431.0
	Final	0.45	0.23	0.57	-19.40	0.34	0.82	786.20	7.18	1.77	295.5
2	Initial	1.12	0.56	1.45	-18.91	0.35	0.82	2862.4	13.1	6.44	347.8
	Final	1.56	0.50	2.99	-24.70	0.46	1.41	6180.4	19.1	13.9	444.2
3	Initial	0.57	0.41	0.50	-18.59	0.33	0.75	1557.2	8.47	3.51	348.8
	Final	0.47	0.28	0.55	-19.46	0.44	1.06	964.50	7.74	2.44	303.3
4	Initial	0.59	0.36	0.60	-21.07	0.34	0.89	1833.6	9.67	4.13	363.0
	Final	0.57	0.32	0.62	-25.52	0.44	1.40	2434.0	10.9	5.48	407.5
5	Initial	0.44	0.28	0.43	-12.16	0.36	0.57	937.55	6.22	2.06	321.3
	Final	0.44	0.26	0.47	-13.21	0.46	0.75	1009.3	6.40	2.27	371.8
Average of all Boulders	Initial	0.75	0.42	0.85	-18.77	0.36	0.85	2283.0	10.8	5.13	362.4
	Final	0.70	0.32	1.04	-20.46	0.43	1.09	2274.9	10.3	5.18	364.5

Note: Symbols are flux-weighted mean residence time (τ_{mean}), flux-weighted median residence time (τ_{50}), flux-weighted standard deviation of residence time (σ_τ), mean downwelling flux (q_d), ratio of downwelling area to total area (A), hyporheic discharge (Q_h), hyporheic volume (V_h), maximum hyporheic depth (D_{max}), mean hyporheic depth (D_{mean}), total hyporheic area (A_h).

[a]Initial and Final indicate the bed condition for the plane bed with boulders before and after sediment transport, respectively. [b]Negative values indicate flux in the downward direction.

Boulder-Scale Hyporheic Flow Spatial Characteristics

Although the effects of bed morphology on residence time of boulder-scale hyporheic flow were not as pronounced as in the reach-scale analysis, the spatial characteristics of hyporheic flow changed between the initial and final scenarios of the boulder-scale analysis. This boulder-scale analysis of hyporheic flow spatial characteristics yielded data that helped determine how changes to bed morphology directly influence how and where water exchanges between surface and subsurface flow in a stream (Figure 7).

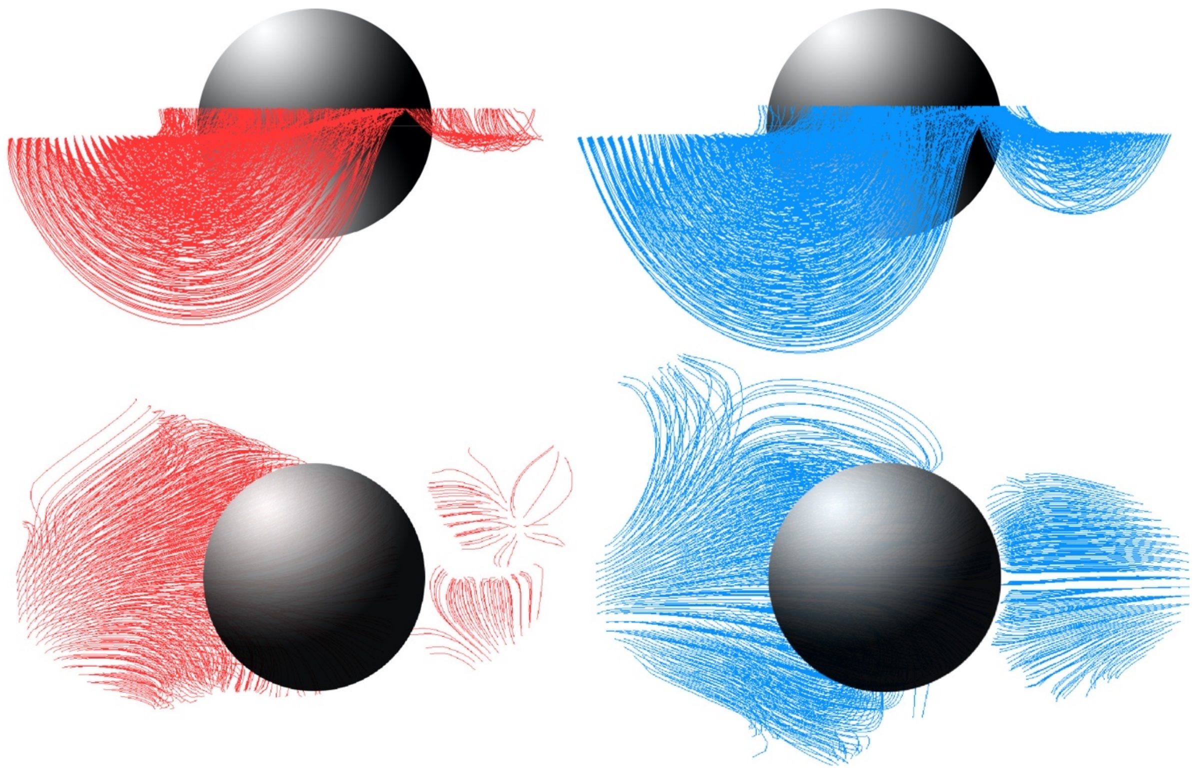

Figure 7. Predicted flowpaths of subsurface flow around boulders for the initial (red) and final (blue) bed conditions at boulder 4 in profile view (top row) and map view (bottom row). Local morphological changes in bed surface elevation create deeper flowpaths and larger hyporheic volume in the final scenario compared to the initial scenario at the boulder-scale. Flow direction is left to right.

Deposition upstream of boulders coupled with downstream erosion increased the local hydraulic head gradients, altered the head distribution around the boulders, and changed the properties of hyporheic flow in the final scenario. Depositional areas along the walls were not included in the boulder-scale analysis because they were outside of the area immediately surrounding the boulder. We observed how the properties of hyporheic flow changed between bed morphologies by comparing the downwelling flux, hyporheic exchange, hyporheic volume, and the spatial distribution of hyporheic flow in the subsurface. The magnitude of mean hyporheic downwelling flux increased near four boulders in the study section. The decrease in mean downwelling flux at boulder 1 is likely attributed to the smallest morphological changes near that boulder (i.e. minimal deposition and erosion upstream and downstream, respectively) between the initial and final scenarios relative to the other boulders. These small morphological changes contributed to the smallest head gradient along the stream-wise distance of boulder 1, while the largest morphological change between the initial and final scenarios occurred at boulders 2 and 4. These large morphological changes increased the head gradient along the stream-wise distance of the boulder, which resulted in the increase in mean downwelling flux. Unlike the reach-scale analysis, the downwelling area in the boulder-scale analysis increased in the final scenarios at boulders 2-5. The near-boulder morphologic changes confined the hyporheic flow to a smaller area on the bed surface due to the increased head gradient along the stream-wise distance of the boulder. Similar to the increase in mean downwelling flux, the mean hyporheic depth increased in the final scenario at boulders 2 and 4 with a small increase at boulder 5. Hyporheic exchange increased near boulders 2-5 in the final scenario. While the mean downwelling flux and downwelling area near boulders 2-5 increased in the final scenario, the hyporheic exchange also increased. This increase of hyporheic exchange in the subsurface consequently resulted in an increase of the maximum hyporheic volume at boulders 2, 4, and 5. The decrease in maximum hyporheic volume at boulders 1 and 3 was due to the decrease in mean depth of hyporheic flow in the final scenario. Similar to boulder 1, boulder 5 exhibited very small morphological changes. In contrast, boulder 1 had larger decreases in residence time and all spatial characteristics of hyporheic flow while boulder 5 exhibited very small changes in residence time and spatial characteristics.

The changes in spatial hyporheic flow characteristics were a direct result of deposition upstream and erosion downstream of the boulders as demonstrated by our results. The topographical adjustment induced an average decrease of τ_{mean} (7%) and τ_{50} (25%), but an increase of σ_t (23%), q_d (9%), and Q_h (28%).

Implications

Practically all mountainous streams and other gravel-bedded morphologies have macro-roughness elements in the form of boulders, large woody debris, or step-pool sequences; therefore, the framework described in this research of coupled large-scale flume experiments and results from numerical modeling are applicable to a wide range of rivers. Results from this research suggest that bedform-scale geomorphic processes are important to consider when macro-roughness elements are present or placed on the streambed and the properties of hyporheic flow are of concern. Local and reach-scale differences in hydraulic head variations resulting from macro-roughness elements are ubiquitous in these systems because streambed morphology adjusts to imposed water and sediment inputs. Therefore, spatial distributions of hyporheic flow properties are expected and must be quantified when obstacles or local changes in bed surface topography alter hydraulic head distributions. Thus, analyses which do not consider the feedback between macro-roughness and streambed morphologic response may not provide the correct quantification of hyporheic exchange. Notice that our results at the reach-scale shows τ_{50} increased by placing the macro-roughness elements but decreased once the streambed morphology reached equilibrium. This underlines that large-scale streambed morphology changes not only impact the magnitude of change but also residence time trends. The addition of boulders blocks 3% of the available surface for shallow hyporheic exchange. This helps explain the increase in median residence time from the original plane bed to initial plane bed with boulders which may have initial implications for bioreactivity before the bed adjust to its final state altering the rate of redox reactions (Pescimoro et al., 2019; Reeder et al., 2018b). Similar to results found in studies examining the effects of low conductivity structures on or near the streambed, we found that boulders placed on the surface restrict down-gradient shallow hyporheic flow and increase the residence time of other flowpaths forced deeper into the subsurface (Pryshlak et al., 2015; Ward et al., 2011). Real rivers are highly complex systems. Including the variability of natural streams in terms of bed surface elevation, roughness sources, and local grain size distribution in a laboratory experiment has many practical challenges. Our experimental configuration, which was implemented in a relatively large-scale flume, is a simplified version of a typical mountain river. However, it captures the most fundamental processes induced by the continuous feedback between the flowing water, sediment transport, and large immobile grains. Allowing the bed surface to freely adjust to the final bed condition is a good representation of a geomorphic response that may be observed in a natural system. We presented a proof-of-concept based only on one case of bed surface elevation change. Other responses in terms of length of residence time and volume of reach-scale hyporheic exchange can be expected under different bed surface configurations or flow characteristics. Future studies should be focused on quantifying these responses of bed and flow properties. We suggest that statistical properties of hyporheic flow metrics would demonstrate similar trends as in our experiments.

The topographical response depends on interactions between flow and macro-roughness elements, sediment inputs, and local grain size distribution. Sawyer et al. (2011) found similar trends as our local-scale analysis for a single channel-spanning log with a mobile streambed and clear-water scour (no sediment input) where hyporheic exchange increased with the presence of macro-roughness elements. The presence of the channel-spanning log created a more extensive head drop due to the blockage of 58% and 67% of the overall flow. They concluded that the impact of streambed adjustments on hyporheic exchange, although visible on the local-scale, was small and the plane bed condition would be sufficient to capture most of the hyporheic flow. This is consistent with our results at the local-scale (hyporheic exchange generated by a single boulder) despite the uniqueness of our experimental setup with localized geometries rather than channel-spanning logs. Conversely, results differ when we consider the induced morphological changes, which extend over a streambed area much larger than the boulder size and cause hyporheic exchange. This could be because boulders in our flume experiments blocked 15% of the flow and had similar contributions to the head gradient as the induced bed adjustments around them. Thus, when multiple macro-roughness elements are present, although sparse, they have a non-linear impact on flow hydraulics, via the momentum and continuity equations, such that local processes may affect the entire reach, which is a result observed in this study. At the reach-scale with sparse macro-roughness elements, the impact of streambed adjustments (final plane bed) is important for hyporheic exchange as downwelling hyporheic discharge nearly doubles while median residence time almost halves from the case with boulders before streambed adjustments (initial plane bed). We argue that, in real streams, macro-roughness elements like boulders, logs or in channel vegetation are rarely found as a single element and, although sparse, they may have a more profound effect on the flow field and streambed morphology that drives hyporheic flows than previously thought. Changes to sediment transport from storm events or land use practices may provide another mechanism to evaluate how hyporheic exchange moves through the shallow subsurface sediments using methods similar to this research. Thus, the feedback between sediment mobility and macro-roughness elements should be accounted for. This could be accomplished by coupling flume experiments with high-resolution computational fluid dynamic modeling.

These hyporheic processes are important for biological activity and strongly influence benthic fauna and riparian vegetation (Krause et al., 2017). For example, understanding how in-stream macro-roughness elements alter the habitat of spawning salmonid species can be useful for implementing low-cost and functional restoration measures (Branco et al., 2013). Results from this study can be capitalized when the goal of restoration efforts are to increase surface and subsurface flow interactions by hyporheic exchange, provide habitat heterogeneity by adding hydraulic complexities from boulders acting as flow obstructions, or recruit spawning fishes to clean and nutrient rich sediments from increased hyporheic exchange. Spawning salmonid species seek clean streambed sediments with adequate flow for their redd locations, which coincide with the hyporheic zone (Baxter & Hauer, 2000). Results indicate that placing macro-roughness elements on the streambed surface alter the morphology which increases the hyporheic exchange delivering nutrients to spawning habitat. This may also have beneficial impacts on nutrient and solute management along streams (Herzog et al., 2016).

The changes in hyporheic flow properties may have important biochemical implications. Reeder et al. (2018a, 2018b) showed that, at flowline resolution, hyporheic reaction kinetics, at least for aerobic respiration (K_{DO}) and anaerobic denitrification (K_{DN}), were linearly proportional to the downwelling velocities of individual flowpaths. Simply stated, faster flowpaths have higher reaction rates. For dune-like structures, flowline velocities are log-normally distributed and so are K_{DO} and K_{DN} as a result. This distribution of reaction rates potentially has some implications for Damköhler-type analyses where a representative residence time (e.g., τ_{50}) is normalized with a reaction rate (e.g., K_{DO} or K_{DN}) (Marzadri et al., 2012; Zarnetske et al., 2012). For an analysis that uses a single-valued reaction rate, how the reaction rate is derived may introduce some bias into the analysis. However, it has been shown that if the single-valued rate is a representative mean or median rate then the analysis will be consistent with a multi-valued analysis. Therefore, boulders and bed adjustments could be expected to increase respiration rates in streambeds, but further observations are needed to test this.

Conclusion

We modeled bed topography and hydraulic head distributions for three key bed morphologies to examine hyporheic flow variations. These data were used to characterize differences in hyporheic flow properties among an original plane gravel streambed, an initial plane gravel streambed with evenly spaced boulders placed on the original plane bed, and the final plane gravel streambed whose morphology adjusted to the imposed flow and sediment inputs with evenly spaced boulders. Each scenario represents a typical geomorphic condition for a natural gravel streambed.

Results show that hyporheic flow depends on various in-stream processes. In-stream macro-roughness elements like immobile boulders are found to influence hyporheic residence time and downwelling flux at local (e.g., near single macro-roughness elements) and reach-scales (e.g., when multiple macro-roughness elements are present). Our results show morphological changes originating and developing from in-stream macro-roughness elements have a greater effect on hyporheic flow compared to solely the in-stream structures. Areas of deposition and erosion developed in each scenario and were generally deterministic for hydraulic head distribution and hyporheic flow direction. These morphological changes, in turn, increased the mean hyporheic flow downwelling flux by nearly 50%, decreased the mean residence time by about 10%, and increased the total hyporheic exchange by nearly 60% for the entire reach after the bed adjusted to the boulders. The geomorphic response at the boulders was not as strong but had a noticeable effect on near-boulder hyporheic exchange. The mean downwelling flux averaged over all the boulders increased by 9% and the median residence time decreased by 25%. More notably, the total hyporheic exchange increased by 28%. Hyporheic residence times tended to be lognormally distributed at the reach-scale (although Kolmogorov-Smirnov goodness-of-fit test was fulfilled only for the initial scenario) and at the local-scale (Kolmogorov-Smirnov goodness-of-fit test was fulfilled at all boulders). Results from this study suggest that geomorphic processes must be carefully considered when modeling hyporheic exchange with macro-roughness elements. Solely placing boulders over plane beds may provide, not only, under or overestimation of hyporheic exchange, but also misleading trends.

References

Abbe, T., & Brooks, A. (2011). Geomorphic, Engineering, and Ecological Considerations when Using Wood in River Restoration. In *Washington DC American Geophysical Union Geophysical Monograph Series* (Vol. 194, pp. 419–451). https://doi.org/10.1029/2010GM001004

Aquaveo L.L.C. (2019). *Groundwater Modeling System*. Provo.

Baxter, C. V., & Hauer, F. R. (2000). Geomorphology, hyporheic exchange, and selection of spawning habitat by bull trout (Salvelinus confluentus). *Canadian Journal of Fisheries and Aquatic Sciences*, *57*(7), 1470–1481. https://doi.org/10.1139/f00-056

Boano, F., Demaria, A., Revelli, R., & Ridolfi, L. (2010). Biogeochemical zonation due to intrameander hyporheic flow. *Water Resources Research*, *46*(2), 1–13. https://doi.org/10.1029/2008WR007583

Boano, F., Harvey, J. W., Marion, A., Packman, A. I., Revelli, R., Ridolfi, L., … Boano F., Harvey J.W., Marion A., Packman A.I., Revelli R.m Ridolfi L., W. A. (2014). Hypohreic flow and transport processes: Mechanisms, models, and biogeochemical implications. *Reviews of Geophysics*, *52*(4), 603–679. https://doi.org/10.1002/2012RG000417.Received

Boulton, A. J., Datry, T., Kasahara, T., Mutz, M., & Stanford, J. A. (2010). Ecology and management of the hyporheic zone: Stream-groundwater interactions of running waters and their floodplains. *Journal of the North American Benthological Society*, *29*(1), 26–40. https://doi.org/10.1899/08-017.1

Branco, P., Boavida, I., Santos, J. M., Pinheiro, A., & Ferreira, M. T. (2013). Boulders as building blocks: Improving habitat and river connectivity for stream fish. *Ecohydrology*, *6*(4), 627–634. https://doi.org/10.1002/eco.1290

Briggs, M. A., Lautz, L. K., Hare, D. K., & González-Pinzón, R. (2013). Relating hyporheic fluxes, residence times, and redox-sensitive biogeochemical processes upstream of beaver dams. *Freshwater Science*, *32*(2), 622–641. https://doi.org/10.1899/12-110.1

Budwig, R., & Goodwin, P. (2012). The Center for Ecohydraulics Research Mountain StreamLab – a facility for collaborative research and education. *Innovations 2012: World Innovations in Engineering Education and Research*.

Buffington, J. M., & Montgomery, D. R. (2013). Geomorphic Classification of Rivers. In J. F. Shroder (Ed.), *Treatise on Geomorphology* (pp. 730–767). https://doi.org/10.1016/B978-0-12-374739-6.00263-3

Cardenas, M. B. (2009). A model for lateral hyporheic flow based on valley slope and channel sinuosity. *Water Resources Research*, *45*(1), 1–5. https://doi.org/10.1029/2008WR007442

Cardenas, M. B., & Wilson, J. L. (2007). Hydrodynamics of coupled flow above and below a sediment-water interface with triangular bedforms. *Advances in Water Resources*, *30*(3), 301–313. https://doi.org/10.1016/j.advwatres.2006.06.009

Cardenas, M. B., Wilson, J. L., & Zlotnik, V. A. (2004). Impact of heterogeneity, bed forms, and stream curvature on subchannel hyporheic exchange. *Water Resources Research*, *40*(8). https://doi.org/10.1029/2004wr003008

Cardenas, M. B., & Zlotnik, V. A. (2003). Three-dimensional model of modern channel bend deposits. *Water Resources Research*, *39*(6), 1–13. https://doi.org/10.1029/2002WR001383

Chen, X., Cardenas, M. B., & Chen, L. (2018). Hyporheic Exchange Driven by Three-Dimensional Sandy Bed Forms: Sensitivity to and Prediction from Bed Form Geometry. *Water Resources Research*, *54*(6), 4131–4149. https://doi.org/10.1029/2018WR022663

Dudunake, T., Tonina, D., Reeder, W. J., & Monsalve, A. (2020). Data from Dudunake et al. (2020), Local and reach-scale hyporheic flow response from boulder induced geomorphic changes, Hydroshare. Retrieved from http://www.hydroshare.org/resource/b3ee375c1559447ba31fbe8319389edb

Elliott, A. H., & Brooks, N. H. (1997). Transfer of nonsorbing solutes to a streambed with bed forms: Laboratory experiments. *Water Resources Research*, *33*(1), 137–151. https://doi.org/10.1029/96wr02783

Endreny, T., Lautz, L., & Siegel, D. I. (2011). Hyporheic flow path response to hydraulic jumps at river steps: Flume and hydrodynamic models. *Water Resources Research*, *47*(2), 1–10. https://doi.org/10.1029/2009WR008631

Ettema, R., Kirkil, G., & Muste, M. (2006). Similitude of Large-Scale Turbulence in Experiments on Local Scour at Cylinders. *Journal of Hydraulic Engineering*, *132*(1), 33–40. Retrieved from http://10.0.4.37/(ASCE)0733-9429(2006)132:1(33)

Gooseff, M. N. (2010). Defining hyporheic zones - advancing our conceptual and operational definitions of where stream water and groundwater meet. *Geography Compass*, *4*(8), 945–955. https://doi.org/10.1111/j.1749-8198.2010.00364.x

Harbaugh, A. W. (2005). *MODFLOW-2005, the US Geological Survey modular ground-water model: the ground-water flow process*. US Department of the Interior, US Geological Survey Reston, VA.

Harvey, Judson W., Gooseff, M. (2015). Consequences From Bedforms To Basins. *Water Resources Research*, *51*(9), 6893–6922. https://doi.org/10.1002/2015WR017617.Received

Harvey, J. W., & Bencala, K. E. (1993). The Effect of streambed topography on surface-subsurface water exchange in mountain catchments. *Water Resources Research*, *29*(1), 89–98. https://doi.org/10.1029/92WR01960

Herzog, S. P., Higgins, C. P., & McCray, J. E. (2016). Engineered streambeds for induced hyporheic flow: Enhanced removal of nutrients, pathogens, and metals from Urban Streams. *Journal of Environmental Engineering (United States)*, *142*(1), 1–10. https://doi.org/10.1061/(ASCE)EE.1943-7870.0001012

Hester, E. T., & Doyle, M. W. (2008). In-stream geomorphic structures as drivers of hyporheic exchange. *Water Resources Research*, *44*(3). https://doi.org/10.1029/2006WR005810

Hester, E. T., Eastes, L. A., & Widdowson, M. A. (2019). Effect of Surface Water Stage Fluctuation on Mixing-Dependent Hyporheic Denitrification in Riverbed Dunes. *Water Resources Research*, *55*(6), 4668–4687. https://doi.org/10.1029/2018WR024198

Hutchinson, P., & Webster, I. (1998). Solute Uptake in Aquatic Sediments due to Current-Obstacle Interactions. *Journal of Environmental Engineering*, *124*(5), 419–426. https://doi.org/10.1061/(ASCE)0733-9372(1998)124:5(419)

Janssen, F., Huettel, M., & Witte, U. (2005). Pore-water advection and solute fluxes in permeable marine sediments (I): Calibration and performance of the novel benthic chamber system Sandy. *Limnology and Oceanography*, *50*(3), 779–792. https://doi.org/10.4319/lo.2005.50.3.0779

Julien, P. Y. (2002). *River mechanics*. Cambridge : Cambridge .

Kang, S., Hill, C., & Sotiropoulos, F. (2016). On the turbulent flow structure around an instream structure with realistic geometry. *Water Resources Research*, *52*(10), 7869–7891. https://doi.org/10.1002/2016WR018688

Kasahara, T., & Wondzell, S. M. (2003). Geomorphic controls on hyporheic exchange flow in mountain streams. *Water Resources Research*, *39*(1), SBH 3-1-SBH 3-14. https://doi.org/10.1029/2002WR001386

Khosronejad, A., Hill, C., Kang, S., & Sotiropoulos, F. (2013). Computational and experimental investigation of scour past laboratory models of stream restoration rock structures. *Advances in Water Resources*, *54*, 191–207. https://doi.org/10.1016/j.advwatres.2013.01.008

Khosronejad, A., Kozarek, J. L., Palmsten, M. L., & Sotiropoulos, F. (2015). Numerical simulation of large dunes in meandering streams and rivers with in-stream rock structures. *Advances in Water Resources*, *81*, 45–61. https://doi.org/10.1016/j.advwatres.2014.09.007

Krause, S., Lewandowski, J., Grimm, N. B., Hannah, D. M., Pinay, G., McDonald, K., … Turk, V. (2017). Ecohydrological interfaces as hot spots of ecosystem processes. *Water Resources Research*, *53*(8), 6359–6376. https://doi.org/10.1002/2016WR019516

Leopold, L. B., & Wolman, M. G. (1957). River Channel Patterns. *Rivers and River Terraces*, 197–237. https://doi.org/10.1007/978-1-349-15382-4_8

Magliozzi, C., Grabowski, R. C., Packman, A. I., & Krause, S. (2018). Toward a conceptual framework of hyporheic exchange across spatial scales. *Hydrology and Earth System Sciences*, *22*(12), 6163–6185. https://doi.org/10.5194/hess-22-6163-2018

Malard, F., Tockner, K., Dole-Olivier, M. J., & Ward, J. V. (2002). A landscape perspective of surface-subsurface hydrological exchanges in river corridors. *Freshwater Biology*, *47*(4), 621–640. https://doi.org/10.1046/j.1365-2427.2002.00906.x

Malcolm, I. A., Soulsby, C., Youngson, A. F., Hannah, D. M., McLaren, I. S., & Thorne, A. (2004). Hydrological influences on hyporheic water quality implications for salmon egg survival. *Hydrological Processes*, *18*(9), 1543–1560. https://doi.org/10.1002/hyp.1405

Marion, A., Bellinello, M., Guymer, I., & Packman, A. (2002). Effect of bed form geometry on the penetration of nonreactive solutes into a streambed. *Water Resources Research*, *38*(10), 27-1-27–12. https://doi.org/10.1029/2001wr000264

Marzadri, A., Dee, M. M., Tonina, D., Bellin, A., & Tank, J. L. (2017). Role of surface and subsurface processes in scaling N2O emissions along riverine networks. *Proceedings of the National Academy of Sciences of the United States of America*, *114*(17), 4330–4335. https://doi.org/10.1073/pnas.1617454114

Marzadri, A., Tonina, D., & Bellin, A. (2012). Morphodynamic controls on redox conditions and on nitrogen dynamics within the hyporheic zone: Application to gravel bed rivers with alternate-bar morphology. *Journal of Geophysical Research: Biogeosciences*, *117*(3), 1–14. https://doi.org/10.1029/2012JG001966

Marzadri, A., Tonina, D., Bellin, A., Vignoli, G., & Tubino, M. (2010). Semianalytical analysis of hyporheic flow induced by alternate bars. *Water Resources Research*, *46*(7), 1–14. https://doi.org/10.1029/2009WR008285

Monsalve, A., & Yager, E. M. (2017). Bed Surface Adjustments to Spatially Variable Flow in Low Relative Submergence Regimes. *Water Resources Research*, *53*(11), 9350–9367. https://doi.org/10.1002/2017WR020845

Monsalve, A., Yager, E. M., & Schmeeckle, M. W. (2017). Effects of Bed Forms and Large Protruding Grains on Near-Bed Flow Hydraulics in Low Relative Submergence Conditions. *Journal of Geophysical Research: Earth Surface*, *122*(10), 1845–1866.

Montgomery, D. R., & Buffington, J. M. (1993). Channel classification, prediction of channel response, and assessment of channel condition. *Washington State Department of Natural Resources Report*, (TFW-SH10-93-002), 84.

Nitsche, M., Rickenmann, D., Turowski, J. M., Badoux, A., & Kirchner, J. W. (2011). Evaluation of bedload transport predictions using flow resistance equations to account for macro-roughness in steep mountain streams. *Water Resources Research*, *47*(8). https://doi.org/10.1029/2011WR010645

ODFW, O. (2010). *Guide to Placement of Wood, Boulders and Gravel for Habitat Restoration*. 33.

Packman, A. I., & Brooks, N. H. (2001). Hyporheic exchange of solutes and colloids with moving bed forms. *Water Resources Research*, *37*(10), 2591–2605. https://doi.org/10.1029/2001WR000477

Payn, R. A., Gooseff, M. N., McGlynn, B. L., Bencala, K. E., & Wondzell, S. M. (2009). Channel water balance and exchange with subsurface flow along a mountain headwater stream in Montana, United States. *Water Resources Research*, *45*(11). https://doi.org/10.1029/2008WR007644

Pescimoro, E., Boano, F., Sawyer, A. H., & Soltanian, M. R. (2019). Modeling Influence of Sediment Heterogeneity on Nutrient Cycling in Streambeds. *Water Resources Research*, *55*(5), 4082–4095. https://doi.org/10.1029/2018WR024221

Pollock, D. W. (2012). *User guide for MODPATH version 6: a particle tracking model for MODFLOW*. US Department of the Interior, US Geological Survey.

Pryshlak, T. T., Sawyer, A. H., Stonedahl, S. H., & Soltanian, M. R. (2015). Multiscale hyporheic exchange through strongly heterogeneous sediments. *Water Resources Research*, *51*(11), 9127–9140.

Reeder, W. J., Quick, A. M., Farrell, T. B., Benner, S. G., Feris, K. P., Marzadri, A., & Tonina, D. (2018a). Hyporheic source and sink of nitrous oxide. *Water Resources Research*, *54*(7), 5001–5016.

Reeder, W. J., Quick, A. M., Farrell, T. B., Benner, S. G., Feris, K. P., & Tonina, D. (2018b). Spatial and Temporal Dynamics of Dissolved Oxygen Concentrations and Bioactivity in the Hyporheic Zone. *Water Resources Research*, *54*(3), 2112–2128. https://doi.org/10.1002/2017WR021388

Rosgen, D. L. (1994). A classification of natural rivers. *Catena*, *22*(3), 169–199.

Sawyer, A. H., Bayani Cardenas, M., & Buttles, J. (2011). Hyporheic exchange due to channel-spanning logs. *Water Resources Research*, *47*(8), 1–12. https://doi.org/10.1029/2011WR010484

Sebok, E., Duque, C., Engesgaard, P., & Boegh, E. (2015). Spatial variability in streambed hydraulic conductivity of contrasting stream morphologies: Channel bend and straight channel. *Hydrological Processes*, *29*(3), 458–472. https://doi.org/10.1002/hyp.10170

Smidt, S. J., Cullin, J. A., Ward, A. S., Robinson, J., Zimmer, M. A., Lautz, L. K., & Endreny, T. A. (2015). A Comparison of Hyporheic Transport at a Cross-Vane Structure and Natural Riffle. *Groundwater*, *53*(6), 859–871. https://doi.org/10.1111/gwat.12288

Stanford, J. A., Lorang, M. S., & Hauer, F. R. (2005). The shifting habitat mosaic of river ecosystems. *SIL Proceedings, 1922-2010*, *29*(1), 123–136. https://doi.org/10.1080/03680770.2005.11901979

Stanford, J. A., & Ward, J. V. (1993). An Ecosystem Perspective of Alluvial Rivers : Connectivity and the Hyporheic Corridor. *Journal of the North American Benthological Society*, *12*(1), 48–60.

Stanford, J. A., & Ward, J. V. (1988). The hyporheic habitat of river ecosystems. *Nature*, *335*(6185), 64–66. https://doi.org/10.1038/335064a0

Stonedahl, S. H., Harvey, J. W., Wörman, A., Salehin, M., & Packman, A. I. (2010). A multiscale model for integrating hyporheic exchange from ripples to meanders. *Water Resources Research*, *46*(12). https://doi.org/10.1029/2009WR008865

Storey, R. G., Howard, K. W. F., & Williams, D. D. (2003). Factors controlling riffle-scale hyporheic exchange flows and their seasonal changes in a gaining stream: A three-dimensional groundwater flow model. *Water Resources Research*, *39*(2), 1–17. https://doi.org/10.1029/2002WR001367

Strom, K. B., Papanicolaou, A. N., & Constantinescu, G. (2007). Case Study: Numerical Modeling of the Tidal Bore on the Qiantang River, China. *Journal of Hydraulic Engineering*, *133*(4), 440–450. https://doi.org/10.1061/(ASCE)0733-9429(2007)133

Thompson, D., & Stull, G. (2002). The Development and Historic Use of Habitat Structures in Channel Restoration in the United States: The Grand Experiment in Fisheries Management. *Geography Physical Quaternaire*, *56*(1), 45–60. https://doi.org/https://doi.org/10.7202/008604ar

Tonina, D., & Buffington, J. M. (2007). Hyporheic exchange in gravel bed rivers with pool-riffle morphology: Laboratory experiments and three-dimensional modeling. *Water Resources Research*, *43*(1), 1–16. https://doi.org/10.1029/2005WR004328

Tonina, D., & Buffington, J. M. (2009). A three-dimensional model for analyzing the effects of salmon redds on hyporheic exchange and egg pocket habitat. *Canadian Journal of Fisheries and Aquatic Sciences*, *66*(12), 2157–2173. https://doi.org/10.1139/F09-146

Trauth, N., Schmidt, C., Maier, U., Vieweg, M., & Fleckenstein, J. H. (2013). Coupled 3-D stream flow and hyporheic flow model under varying stream and ambient groundwater flow conditions in a pool-riffle system. *Water Resources Research*, *49*(9), 5834–5850. https://doi.org/10.1002/wrcr.20442

Ward, A. S., Gooseff, M. N., & Johnson, P. A. (2011). How can subsurface modifications to hydraulic conductivity be designed as stream restoration structures? Analysis of Vaux's conceptual models to enhance hyporheic exchange. *Water Resources Research*, *47*(8), 1–13. https://doi.org/10.1029/2010WR010028

Weller, H. G., Tabor, G., Jasak, H., & Fureby, C. (1998). A tensorial approach to computational continuum mechanics using object-oriented techniques. *Computers in Physics*, *12*(6), 620. https://doi.org/10.1063/1.168744

Yager, E. M., Kirchner, J. W., & Dietrich, W. E. (2007). Calculating bed load transport in steep boulder bed channels. *Water Resources Research*, *43*(7). https://doi.org/10.1029/2006wr005432

Yager, E. M., & Schmeeckle, M. W. (2013). The influence of vegetation on turbulence and bed load transport. *Journal of Geophysical Research: Earth Surface*, *118*(3), 1585–1601. https://doi.org/10.1002/jgrf.20085

Zaramella, M., Packman, A. I., & Marion, A. (2003). Application of the transient storage model to analyze advective hyporheic exchange with deep and shallow sediment beds. *Water Resources Research*, *39*(7), 1–12. https://doi.org/10.1029/2002WR001344

Zarnetske, J. P., Haggerty, R., Wondzell, S. M., Bokil, V. A., & González-Pinzón, R. (2012). Coupled transport and reaction kinetics control the nitrate source-sink function of hyporheic zones. *Water Resources Research*, *48*(11), 1–15. https://doi.org/10.1029/2012WR011894

Zimmermann, A. E., & Lapointe, M. (2005). Intergranular flow velocity through salmonid redds: Sensitivity to fines infiltration from low intensity sediment transport events. *River Research and Applications*, *21*(8), 865–881. https://doi.org/10.1002/rra.856

Appendix

Appendix 1: Letter of Permission from Publisher

JOHN WILEY AND SONS LICENSE
TERMS AND CONDITIONS

Oct 24, 2020

This Agreement between Taylor Dudunake ("You") and John Wiley and Sons ("John Wiley and Sons") consists of your license details and the terms and conditions provided by John Wiley and Sons and Copyright Clearance Center.

License Number	4935490465617
License date	Oct 24, 2020
Licensed Content Publisher	John Wiley and Sons
Licensed Content Publication	Water Resources Research
Licensed Content Title	Local and Reach−Scale Hyporheic Flow Response From Boulder−Induced Geomorphic Changes
Licensed Content Author	T. Dudunake, D. Tonina, W. J. Reeder, et al
Licensed Content Date	Oct 13, 2020
Licensed Content Volume	56
Licensed Content Issue	10

Licensed Content Pages	15
Type of use	Dissertation/Thesis
Requestor type	Author of this Wiley article
Format	Print and electronic
Portion	Full article
Will you be translating?	No
Title	Effects of Boulders on Bed Morphology and Hyporheic Flow
Institution name	University of Idaho
Expected presentation date	Dec 2020
Requestor Location	Taylor Dudunake 2356 E. Cougar Creek St. MERIDIAN, ID 83646 United States Attn: Taylor Dudunake
Publisher Tax ID	EU826007151
Total	0.00 USD

Terms and Conditions

TERMS AND CONDITIONS

This copyrighted material is owned by or exclusively licensed to John Wiley & Sons, Inc. or one of its group companies (each a"Wiley Company") or handled on behalf of a society with which a Wiley Company has exclusive publishing rights in relation to a particular work (collectively "WILEY"). By clicking "accept" in connection with completing this licensing transaction, you agree that the following terms and conditions apply to this transaction (along with the billing and payment terms and conditions established by the Copyright Clearance Center Inc., ("CCC's Billing and Payment terms and conditions"), at the time that you opened your RightsLink account (these are available at any time at http://myaccount.copyright.com).

Terms and Conditions

- The materials you have requested permission to reproduce or reuse (the "Wiley Materials") are protected by copyright.
- You are hereby granted a personal, non-exclusive, non-sub licensable (on a stand-alone basis), non-transferable, worldwide, limited license to reproduce the Wiley Materials for the purpose specified in the licensing process. This license, **and any CONTENT (PDF or image file) purchased as part of your order,** is for a one-time use only and limited to any maximum distribution number specified in the license. The first instance of republication or reuse granted by this license must be completed within two years of the date of the grant of this license (although copies prepared before the end date may be distributed thereafter). The Wiley Materials shall not be used in any other manner or for any other purpose, beyond what is granted in the license. Permission is granted subject to an appropriate acknowledgement given to the author, title of the material/book/journal and the publisher. You shall also duplicate the copyright notice that appears in the Wiley publication in your use of the Wiley Material. Permission is also granted on the understanding that nowhere in the text is a previously published source acknowledged for all or part of this Wiley Material. Any third party content is expressly excluded from this permission.
- With respect to the Wiley Materials, all rights are reserved. Except as expressly granted by the terms of the license, no part of the Wiley Materials may be copied, modified, adapted (except for minor reformatting required by the new Publication), translated, reproduced, transferred or distributed, in any form or by any means, and no derivative works may be made based on the Wiley Materials without the prior permission of the respective copyright owner.**For STM Signatory Publishers clearing permission under the terms of the STM Permissions Guidelines only, the terms of the license are extended to include subsequent editions and for editions in other languages, provided such editions are for the work as a whole in situ and does not involve the separate exploitation of the permitted figures or extracts,**

You may not alter, remove or suppress in any manner any copyright, trademark or other notices displayed by the Wiley Materials. You may not license, rent, sell, loan, lease, pledge, offer as security, transfer or assign the Wiley Materials on a stand-alone basis, or any of the rights granted to you hereunder to any other person.

- The Wiley Materials and all of the intellectual property rights therein shall at all times remain the exclusive property of John Wiley & Sons Inc, the Wiley Companies, or their respective licensors, and your interest therein is only that of having possession of and the right to reproduce the Wiley Materials pursuant to Section 2 herein during the continuance of this Agreement. You agree that you own no right, title or interest in or to the Wiley Materials or any of the intellectual property rights therein. You shall have no rights hereunder other than the license as provided for above in Section 2. No right, license or interest to any trademark, trade name, service mark or other branding ("Marks") of WILEY or its licensors is granted hereunder, and you agree that you shall not assert any such right, license or interest with respect thereto

- NEITHER WILEY NOR ITS LICENSORS MAKES ANY WARRANTY OR REPRESENTATION OF ANY KIND TO YOU OR ANY THIRD PARTY, EXPRESS, IMPLIED OR STATUTORY, WITH RESPECT TO THE MATERIALS OR THE ACCURACY OF ANY INFORMATION CONTAINED IN THE MATERIALS, INCLUDING, WITHOUT LIMITATION, ANY IMPLIED WARRANTY OF MERCHANTABILITY, ACCURACY, SATISFACTORY QUALITY, FITNESS FOR A PARTICULAR PURPOSE, USABILITY, INTEGRATION OR NON-INFRINGEMENT AND ALL SUCH WARRANTIES ARE HEREBY EXCLUDED BY WILEY AND ITS LICENSORS AND WAIVED BY YOU.

- WILEY shall have the right to terminate this Agreement immediately upon breach of this Agreement by you.

- You shall indemnify, defend and hold harmless WILEY, its Licensors and their respective directors, officers, agents and employees, from and against any actual or threatened claims, demands, causes of action or proceedings arising from any breach of this Agreement by you.

- IN NO EVENT SHALL WILEY OR ITS LICENSORS BE LIABLE TO YOU OR ANY OTHER PARTY OR ANY OTHER PERSON OR ENTITY FOR ANY SPECIAL, CONSEQUENTIAL, INCIDENTAL, INDIRECT, EXEMPLARY OR PUNITIVE DAMAGES, HOWEVER CAUSED, ARISING OUT OF OR IN CONNECTION WITH THE DOWNLOADING, PROVISIONING, VIEWING OR USE OF THE MATERIALS REGARDLESS OF THE FORM OF ACTION, WHETHER FOR BREACH OF CONTRACT, BREACH OF WARRANTY, TORT, NEGLIGENCE, INFRINGEMENT OR OTHERWISE (INCLUDING, WITHOUT LIMITATION, DAMAGES BASED ON LOSS OF PROFITS, DATA, FILES, USE, BUSINESS OPPORTUNITY OR CLAIMS OF THIRD PARTIES), AND WHETHER OR NOT THE PARTY HAS BEEN ADVISED OF THE POSSIBILITY OF SUCH DAMAGES. THIS LIMITATION SHALL APPLY NOTWITHSTANDING ANY

FAILURE OF ESSENTIAL PURPOSE OF ANY LIMITED REMEDY PROVIDED HEREIN.

- Should any provision of this Agreement be held by a court of competent jurisdiction to be illegal, invalid, or unenforceable, that provision shall be deemed amended to achieve as nearly as possible the same economic effect as the original provision, and the legality, validity and enforceability of the remaining provisions of this Agreement shall not be affected or impaired thereby.

- The failure of either party to enforce any term or condition of this Agreement shall not constitute a waiver of either party's right to enforce each and every term and condition of this Agreement. No breach under this agreement shall be deemed waived or excused by either party unless such waiver or consent is in writing signed by the party granting such waiver or consent. The waiver by or consent of a party to a breach of any provision of this Agreement shall not operate or be construed as a waiver of or consent to any other or subsequent breach by such other party.

- This Agreement may not be assigned (including by operation of law or otherwise) by you without WILEY's prior written consent.

- Any fee required for this permission shall be non-refundable after thirty (30) days from receipt by the CCC.

- These terms and conditions together with CCC's Billing and Payment terms and conditions (which are incorporated herein) form the entire agreement between you and WILEY concerning this licensing transaction and (in the absence of fraud) supersedes all prior agreements and representations of the parties, oral or written. This Agreement may not be amended except in writing signed by both parties. This Agreement shall be binding upon and inure to the benefit of the parties' successors, legal representatives, and authorized assigns.

- In the event of any conflict between your obligations established by these terms and conditions and those established by CCC's Billing and Payment terms and conditions, these terms and conditions shall prevail.

- WILEY expressly reserves all rights not specifically granted in the combination of (i) the license details provided by you and accepted in the course of this licensing transaction, (ii) these terms and conditions and (iii) CCC's Billing and Payment terms and conditions.

- This Agreement will be void if the Type of Use, Format, Circulation, or Requestor Type was misrepresented during the licensing process.

- This Agreement shall be governed by and construed in accordance with the laws of the State of New York, USA, without regards to such state's conflict of law rules. Any legal action, suit or proceeding arising out of or relating to these Terms and Conditions or the breach thereof shall be instituted in a court of competent jurisdiction in New

York County in the State of New York in the United States of America and each party hereby consents and submits to the personal jurisdiction of such court, waives any objection to venue in such court and consents to service of process by registered or certified mail, return receipt requested, at the last known address of such party.

WILEY OPEN ACCESS TERMS AND CONDITIONS

Wiley Publishes Open Access Articles in fully Open Access Journals and in Subscription journals offering Online Open. Although most of the fully Open Access journals publish open access articles under the terms of the Creative Commons Attribution (CC BY) License only, the subscription journals and a few of the Open Access Journals offer a choice of Creative Commons Licenses. The license type is clearly identified on the article.

The Creative Commons Attribution License

The Creative Commons Attribution License (CC-BY) allows users to copy, distribute and transmit an article, adapt the article and make commercial use of the article. The CC-BY license permits commercial and non-

Creative Commons Attribution Non-Commercial License

The Creative Commons Attribution Non-Commercial (CC-BY-NC)License permits use, distribution and reproduction in any medium, provided the original work is properly cited and is not used for commercial purposes.(see below)

Creative Commons Attribution-Non-Commercial-NoDerivs License

The Creative Commons Attribution Non-Commercial-NoDerivs License (CC-BY-NC-ND) permits use, distribution and reproduction in any medium, provided the original work is properly cited, is not used for commercial purposes and no modifications or adaptations are made. (see below)

Use by commercial "for-profit" organizations

Use of Wiley Open Access articles for commercial, promotional, or marketing purposes requires further explicit permission from Wiley and will be subject to a fee.

Further details can be found on Wiley Online Library
http://olabout.wiley.com/WileyCDA/Section/id-410895.html

Other Terms and Conditions:

v1.10 Last updated September 2015

Questions? customercare@copyright.com or +1-855-239-3415 (toll free in the US) or +1-978-646-2777.